# A membrane model for cytosolic calcium oscillations

## A study using *Xenopus* oocytes

M. Saleet Jafri,[‡] Sandor Vajda,[§] Pedro Pasik,[‖] and Boaz Gillo*

*Department of Neurology and Fishberg Research Center for Neurobiology, and [‡]Department of Biomathematical Sciences, Mount Sinai School of Medicine, New York, New York 10029 USA; [§]Department of Biomedical Engineering, Boston University, Boston, Massachusetts 02215 USA; and [‖]Department of Neurology and Department of Cell Biology and Anatomy, Mount Sinai School of Medicine, New York, New York 10029 USA

ABSTRACT Cytosolic calcium oscillations occur in a wide variety of cells and are involved in different cellular functions. We describe these calcium oscillations by a mathematical model based on the putative electrophysiological properties of the endoplasmic reticulum (ER) membrane. The salient features of our membrane model are calcium-dependent calcium channels and calcium pumps in the ER membrane, constant entry of calcium into the cytosol, calcium dependent removal from the cytosol, and buffering by cytoplasmic calcium binding proteins. Numerical integration of the model allows us to study the fluctuations in the cytosolic calcium concentration, the ER membrane potential, and the concentration of free calcium binding sites on a calcium binding protein. The model demonstrates the physiological features necessary for calcium oscillations and suggests that the level of calcium flux into the cytosol controls the frequency and amplitude of oscillations. The model also suggests that the level of buffering affects the frequency and amplitude of the oscillations. The model is supported by experiments indirectly measuring cytosolic calcium by calcium-induced chloride currents in *Xenopus* oocytes as well as cytosolic calcium oscillations observed in other preparations.

## INTRODUCTION

Oscillations in the cytosolic calcium concentration ($[Ca]_{cyt}$) regulate a variety of cellular functions in different systems, such as the secretion in the pituitary (Schlegal et al., 1987) and parotid glands (Gray, 1988), the contraction of smooth muscle (Ambler et al., 1988; Benham et al., 1986), and cardiac inotrophy and induction of arrhythmias (Lakatta et al., 1986). These oscillations also occur in cells where their function remains unknown, such as fibroblasts (Harootunian et al., 1988), endothelial cells (Jacob et al., 1988), and oocytes (Gillo et al., 1987; DeLisle et al., 1990). Experimentally, calcium oscillations are evoked through the application of extracellular calcium (Harootunian et al., 1988; Stern et al., 1988) or calcium mobilizing neurotransmitters (Wakui and Petersen, 1990). These stimuli are responsible for calcium entry into the cytosol through plasmalemmal calcium channels or release from intracellular stores mediated by a secondary messenger, such as inositol trisphosphate ($IP_3$; Berridge and Irvine, 1989).

Recently, two classes of mathematical models have been proposed to explain the mechanism for cytosolic calcium oscillations: (*a*) a molecular model (Meyer and Stryer, 1988; Swillens and Mercan, 1990) which uses $IP_3$ binding as the driving force behind the oscillations, and (*b*) a compartmental calcium-exchange model (Kuba and Takeshita, 1981; Goldbeter et al., 1990; Somogyi and Stucki, 1991) which is based on the fluctuations in the calcium concentration in both the cytosol and the ER lumen. The model proposed by Goldbeter and coworkers (1990) adds a constant calcium flux into the cytosol from $IP_3$-sensitive stores. It relies on the balance between the cytosolic and ER luminal calcium so that the depletion of the latter causes the closing of the ER calcium channel, thereby inhibiting the calcium-dependent calcium release. The formulation by Somogyi and Stucki (1991) differs from the original compartmental calcium-exchange model in that it requires cooperative binding of $IP_3$ and calmodulin to the ER calcium release channel.

We propose another possible physiological mechanism to explain calcium oscillations which is based on the interplay between the calcium channels and the calcium pumps in the ER membrane. Okada and coworkers (1982) offered a similar mechanism in which the calcium oscillations occurred as a result of the movement of calcium across the plasma membrane. Jacob and co-workers (1988), however, showed that in certain cells the plasma membrane potential played no role in cytosolic calcium oscillations, although they did not exclude the role of ER membrane potential fluctuations. In our model, the driving force behind the oscillations is the electrochemical gradient across the ER membrane. Calcium oscillations would occur when the elevation in cytosolic calcium triggers calcium-dependent calcium release from the ER. The rate of release will increase autocatalytically due to the additional increase in cytosolic calcium. The termination of release occurs when the electrochemical gradient of calcium is diminished by the increase of cytosolic calcium so that the rate of calcium removal by the action of calcium pumps exceeds the rate of movement of calcium through the channel. Since the pump rate is dependent on calcium binding, as the cytosolic calcium concentration decreases the pump rate also decreases. Eventually, the pump rate will fall enough so that the calcium entry into the cytosol once again dominates the changes in cytosolic calcium. This cycle repeats itself and oscillations occur. It is important to note that the cytosolic calcium entry that triggers these events is constant and need not oscillate.

Address correspondence to M. Saleet Jafri, Department of Biomathematical Sciences, Box 1023, Mount Sinai School of Medicine, New York, NY 10029.


0006-3495/92/07/235/12 $2.00

In this study, we present our membrane model as a different mechanism to describe cytosolic calcium oscillations by means of equations that represent the changes in cytosolic calcium and ER membrane potential. In addition, we simulate the potential role of buffering in the control of cytoplasmic calcium oscillations. The model is applied to simulate calcium-evoked chloride current oscillations in *Xenopus* oocytes and may also explain calcium oscillations in other systems.

## THE MODEL

### Glossary of terms

#### Variables

$[Ca]_{cyt}$ = cytosolic calcium concentration
$[P]$ = concentration of buffer protein binding sites
$V$ = ER membrane potential

#### Functions

$I_{Ca}$ = calcium current through ER channel
$E_{Ca}$ = reversal potential across ER for calcium

#### Parameters

$R$ = ideal gas constant
$T$ = absolute temperature
$F$ = Faraday's constant
$[Ca]_{ER}$ = ER calcium concentration
$g_{Ca}$ = calcium conductance through ER calcium channel per area
$\overline{g_{Ca}}$ = maximal calcium conductance per area
$S$ = surface area of ER membrane
$K_{diss}$ = dissociation constant off channel protein
$V_{cyt}$ = volume of cytosolic compartment
$k_{pump}$ = pump rate into the ER
$k$ = pump rate out of cytosol
$q$ = flux of calcium into cytosol
$C_m$ = ER membrane capacitance per area
$k_{off}$ = off rate for buffer protein binding sites
$k_{on}$ = on rate for buffer protein binding sites
$[P_{total}]$ = total concentration of buffer protein binding sites

The model is based on the following assumptions: (*a*) The ER membrane is excitable, that is, it separates charge and has ionic currents flowing across it. Calcium is the only ion that significantly contributes capacitative current to evoke changes in the ER membrane potential. (*b*) The plasma membrane potential has no influence on the oscillations (Jacob et al., 1988; Harootunian et al., 1988). (*c*) The oscillations occur as a result of competition between the calcium-dependent calcium release from the ER and the uptake from the cytosol into the ER by a calcium-dependent pump. (*d*) There is a constant calcium entry into the cytosol from either intracellular sources through calcium release mediated by a second messenger, such as $IP_3$, or extracellular sources through plasma membrane calcium channels. (*e*) There is calcium-dependent efflux from the cytosol into the extracellular space by a plasmalemmal calcium pump. (*f*) The calcium oscillations in *Xenopus* oocytes that are measured by the calcium-dependent chloride current in the plasma membrane occur primarily in a cytosolic compartment which is approximated by a spherical shell comprised of the outer 1 $\mu$m of the oocyte (see section on electron microscopy and stereology). (*g*) Cytosolic calcium is bound by calcium binding proteins.

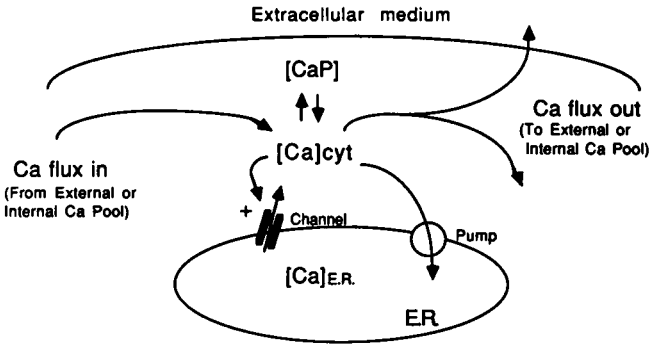


FIGURE 1 Schematic representation of the calcium oscillation components involved in the membrane model. Notice that an increase in $[Ca]_{cyt}$ triggers calcium release from the ER. The calcium bound to cytosolic calcium binding proteins is represented by [CaP].

The oocyte has a complex buffering system consisting of calcium binding proteins and calcium stores. The main cytosolic calcium binding protein is calmodulin which has a binding constant of $10^{-6}$ $M^{-1}$ (Robertson et al., 1981). Calmodulin has four calcium binding sites that herein are treated as independent sites. The balance equation for free calmodulin is given by

$$\frac{d[P]}{dt} = k_{off}([P_{total}] - [P]) - k_{on}([Ca]_{cyt}[P]), \qquad (1)$$

where $[P]$ is the concentration of free calmodulin calcium binding sites, $[P_{total}]$ is the total amount of calmodulin calcium binding sites in the cell, $[Ca]_{cyt}$ is the cytosolic calcium concentration, and $k_{on}$ and $k_{off}$ are the on and off rates from the binding sites. The concentration of calmodulin in a resting *Xenopus* oocyte is $\sim$34 $\mu$M (Cartaud et al., 1980). Calmodulin has four binding sites per molecule which yields a total of $\sim$132 $\mu$M calcium binding sites. We use 120 $\mu$M as the total amount of calcium binding sites. The dissociation constant of calcium from calmodulin ranges from 0.2 to 18 $\mu$M (Robertson et al., 1981; Lin et al., 1974; Wolff et al., 1977). We use a value of 1 $\mu$M with 5 $\mu M^{-1}$ $s^{-1}$ for $k_{on}$ and 5 $s^{-1}$ for $k_{off}$.

The membrane model assumes that the ER membrane has electrophysiological properties similar to the plasma membrane. The ER membrane is depolarized by the calcium current and repolarized by the calcium pump (Fig. 1).

The calcium current across the ER membrane is given by

$$I_{Ca} = g_{Ca}(E_{Ca} - V), \quad (2)$$

where $g_{Ca}$ is the ER membrane calcium conductance per unit area, $E_{Ca}$ is the reversal potential for calcium, and $V$ is the potential difference across the ER. For simplicity, we assume that the ER luminal calcium concentration ($[Ca]_{ER}$) remains constant at 5 mM (Somlyo et al., 1981). The reversal potential for calcium ($E_{Ca}$) is calculated by using the Nernst equation

$$E_{Ca} = \frac{RT}{zF} \ln\left(\frac{[Ca]_{ER}}{[Ca]_{cyt}}\right). \quad (3)$$

Data on the ER calcium channel is derived from experiments on the sarcoplasmic reticulum (SR) because no such information is available on the ER. The conductance is simplified (Eq. 4) as cooperative binding given by Hill's equation with Hill coefficient $n = 2$ (Meissner et al., 1986; Chay and Keizer, 1983). The concentration of SR luminal calcium (*trans*) has been shown to have no effect on the duration of channel opening (Lai et al., 1988). Thus, there is no inhibition by *trans* calcium. It has also been shown that highly elevated *cis* calcium (>10 $\mu$M) inhibits calcium release through this channel (Meissner et al., 1986). However, this calcium concentration is above the physiological values observed during calcium oscillations and may contribute to the inhibition of the calcium oscillations at high calcium levels. In our model, we attribute the inhibition by high *cis* calcium to the decrease of the electrochemical gradient. Hence, the conductance is given by

$$g_{Ca} = \overline{g_{Ca}} S \frac{\left(\frac{[Ca]_{cyt}}{K_{diss}}\right)^2}{1 + \left(\frac{[Ca]_{cyt}}{K_{diss}}\right)^2}, \quad (4)$$

where $\overline{g_{Ca}}$ is the maximal ER membrane conductance per unit area, and $S$ is the ER surface area (see below). The dissociation constant of calcium from the channel protein is represented by $K_{diss}$. $K_{diss}$ should be in the range of 2–10 $\mu$M (Meissner et al., 1986). We choose a value of 5 $\mu$M for $K_{diss}$.

The pump is assumed to depend linearly on the $[Ca]_{cyt}$ because the physiological range is on the linear part of the Michaelis-Menten curve (Ogawa et al., 1981; Gandhi and Ross, 1988). In Eq. 5 below, $k_{pump}$ is the pump rate from the cytosol into the ER. Ogawa and co-workers (1981) measured a maximal pump rate of 69.8 mM $s^{-1}$ with a $K_m$ of 1 $\mu$M for SR calcium uptake in frog skeletal muscle. The rate constant calculated when $[Ca]_{cyt}$ is 1 $\mu$M is 250 $s^{-1}$. For the oocyte, the rate constant will be considerably slower, i.e., 20.2 $s^{-1}$ because the oscillations are slow compared with those occurring during a muscle twitch.

We can now write the complete balance equation for $[Ca]_{cyt}$

$$\frac{d[Ca]_{cyt}}{dt} = \frac{I_{Ca}}{2FV_{cyt}} - k_{pump}[Ca]_{cyt} + \frac{q}{V_{cyt}} - k[Ca]_{cyt} + k_{off}([P_{total}] - [P]) - k_{on}[Ca]_{cyt}[P], \quad (5)$$

where $V_{cyt}$ is the cytosolic compartment volume (see below), $k$ is the rate constant of calcium efflux from the cytosol across the plasma membrane, and $F$ is Faraday's constant. The factor 2 in the denominator is the charge on a calcium ion. The calcium flux $q$ into the cytosol remains constant during the course of an oscillation. In different simulations, which are described in the results, the value of $q$ is varied to produce different behavior.

The second equation for the model, that of the ER membrane potential, is given by

$$SC_m \frac{dV}{dt} = I_{Ca} - 2FV_{cyt}k_{pump}[Ca]_{cyt}, \quad (6)$$

where $C_m$ is the membrane capacitance per unit area and $V$ is the potential difference across the membrane. The first term on the right hand side of the equation is the capacitative current due to calcium movement through the channel. The second term is the electrogenic current generated by the ER calcium pump. The complete model is given in Eqs. 1 through 6.

## EXPERIMENTAL PROCEDURES

### Materials

Collagenase type 1A and other reagents and chemicals were obtained from Sigma Chemical Co. (St. Louis, MO).

### Oocyte culture

*Xenopus laevis* (Xenopus One; Ann Arbor, MI or NASCO, Ft. Atkinson, WI) were maintained at 18–20°C and a day–night cycle of 15 h/9 h. A section of ovary was removed surgically from female frogs under percutaneous tricaine anesthesia and the oocytes defolliculated for 2 h with 2 mg/ml collagenase in calcium-free ND96 solution (96 mM NaCl, 2 mM KCl, 1 mM $MgCl_2$, 5 mM Hepes, pH = 7.5). Oocytes were examined under a dissecting microscope, and healthy looking stage V and stage VI cells (Dumont, 1972) were selected and maintained at 21°C in enriched ND96 (supplemented with 1.8 mM $CaCl_2$, 2.5 mM sodium phosphate, 100 U/ml penicillin and 100 $\mu$g/ml streptomycin) for 1–3 d before recording.

### Electrophysiology

Cells were placed in a 0.5-ml bath which was constantly perfused with medium and then penetrated with two 0.5–1 MΩ, 3 M KCL filled glass electrodes attached to a DAGAN 8500 amplifier, using an 8100 probe (Dagan Corp., Minneapolis, MN). An IBM PC/AT system employing the TL-1 interface and pClamp software from Axon Instruments (Burlingame, CA) was used for maintaining voltage-clamp conditions. Cells were usually held at −70 mV unless otherwise stated. The current in the voltage-clamp circuit was registered on a chart recorder (Yokogawa, Tokyo, Japan).

The composition of the "calcium-free medium" used to incubate and perfuse the oocytes was 86 mM NaCl, 2 mM KCl, 15 mM $MgCl_2$, 0.2 mM EGTA, and 5 mM Hepes, pH = 7.5. For acute application of calcium, 5 mM $CaCl_2$ was substituted for 5 mM $MgCl_2$ (no EGTA) to

maintain the osmolarity unchanged. This solution is referred to as "calcium-containing medium."

## Intracellular application of substances

Two techniques were used to introduce reagents into the oocyte cytosol. For acute calcium injection, hereby referred to as "injection," a pressure system was used. For this purpose, a cell under voltage-clamp had a third micropipette introduced. Pipettes were obtained by breaking the tip to 2–4 $\mu$m diameter under microscopic control. The 50-mM calcium solution was introduced into the pipette tip by applying negative pressure to the open side. The filled pipette was connected by a rigid tube to a controller which delivered pulses of compressed nitrogen for specified time intervals (Picospritzer II; General Valve Corp., Fairfield, NJ). Before insertion into and after withdrawal from the cell, the pipette tip was immersed in a drop of mineral oil and observed under a microscope with an eye piece micrometer. The pressure was adjusted to obtain a drop of drug with a volume of less than 0.4% of the volume of the oocyte (100–200 $\mu$m diameter which is equivalent to 50–200 pmol/cell). From the calcium concentration and the drop diameter the amount of calcium actually injected could be determined.

Preloading the cell (>10 min exposure) with $IP_3$, referred to as "loading," was made with a microdispenser (Drumond, Broomall, PA) through a pulled glass capillary tube with the tip broken at 10 $\mu$m diameter. A drop of mineral oil was added to the tube before introduction of the microdispenser plunger, and 1–2 $\mu$l solution was added by backfilling. 30 to 50 nl of the solution were introduced into the cells after penetration.

## Electron microscopy and stereology

Recent development of microfluorescence measurement of calcium signals in *Xenopus* oocytes found that maximal fluorescence intensity is recorded ~10 $\mu$m beneath the plasmalemma (Takehashi et al., 1987). In fact, calcium oscillations were observed 5 $\mu$m below the surface membrane (Parker and Ivorra, 1990). In our work, we monitor the changes in cytosolic calcium using the native calcium-sensitive chloride channel. Thus, we assume that changes in calcium concentration occur in the submembranal region. Deep injections of calcium over 100 $\mu$m deep (see Experimental section below) do not immediately activate the chloride channels. This suggests that the measured calcium oscillations are a result of calcium elevation closer to the membrane. Taken together, we confine our analysis of the cytosolic volume and the ER surface area to the cytosolic compartment, that is, the volume of the cytosol close to the plasma membrane. We assume that it well represents the region where the calcium oscillations occur.

Immature denuded oocytes were prepared for transmission electron microscopy prepared according to published protocols (Gardiner and Grey, 1983; Charbonneau and Grey, 1984). Oocytes were fixed for 2 h in 2.5% glutaraldehyde in ND96 at 4°C, then washed and cut by fine scalpel into the two hemispheres. Only animal hemispheres were used, as it is known that they contain the larger number of Ca mobilizing related components (Gardiner and Grey, 1983). Animal hemispheres were post-fixed for 1 h in 1% $OsO_4$ in 50% ND96 at 4°C. After washing in buffer, specimens were dehydrated in graded ethanol with 1% uranyl acetate in the 70% stage. Finally, they were embedded in Epon-Araldite with the equatorial face resting on the flat embedding vessel. After polymerization, the specimen was glued on its side on a blank resin block and sectioned perpendicular to the flat face. Ultrathin sections (silver interference color) were collected on formvar-coated slot grids, after discarding the first 400 $\mu$m. In this way, sections were taken from the equatorial region of the animal hemisphere. After counterstaining with uranyl and lead salts, grids were examined with a Hitachi 12A electron microscope and micrographs taken at 12,000 magnification and further enlarged in printing to 30,000 magnification (Plate 1).

The cytosolic compartment consists of the region between the cortical granules and the plasma membrane which is approximated by a spherical shell ~1 $\mu$m in thickness. Its volume ($W$) is easily estimated using the difference in volume of two spheres

$$W = \left(\frac{4\pi}{3}\right)(r^3 - (r-1)^3), \tag{7}$$

where $r$ is the cell radius.

The value of the ER surface area ($S$) is derived from area and length measurements on the electron micrographs obtained through planimetry and the application of the fundamental stereologic principle. The fundamental stereologic principle (Delesse, 1847) states that the fraction $V_1$ of a volume $V_2$ occupied by randomly distributed components is equal to the fraction $A_1$ of the area $A_2$ of a plane of section of volume $V_2$ covered by transections of those components, that is,

$$\frac{A_1}{A_2} = \frac{V_1}{V_2}. \tag{8}$$

The following morphometric measurements were made on the oocyte cortical cytosol appearing in four electron micrographs:

$a_{tot}$ = total cross-sectional area of the cortical cytosol (area between the cortical granules and the plasma membrane including the ER);

$a_{ER}$ = cumulative cross-sectional area of the ER in the cortical cytosol;

$L_{ER}$ = cumulative long axes of the ER cisterns in the cortical cytosol.

The following calculations were made to estimate the ER surface area to cytosolic volume ratio:

$$a_{cyt} = a_{tot} - a_{ER}, \tag{9}$$

where $a_{cyt}$ is the area of the cortical cytosol. Then,

$$r_{mean} = \frac{1}{2}\frac{a_{ER}}{L_{ER}}, \tag{10}$$

where $r_{mean}$ is the mean radius of ER cisterns, and

$$v_{ER} = \frac{\pi a_{ER}^2}{4L_{ER}}, \tag{11}$$

where $v_{ER}$ is the take volume of the ER. The surface area of the ER is given by

$$s_{ER} = \pi a_{ER} + n\frac{\pi a_{ER}^2}{4L_{ER}^2}, \tag{12}$$

where $n$ is the number of ER cisterns present in the sample. Using the fundamental stereologic principle, the cytosolic volume in the sample is

$$v_{cyt} = \frac{a_{cyt}v_{ER}}{a_{ER}}. \tag{13}$$

Finally, the value of the ER surface area (Table 1) for the entire compartment is

$$S = \frac{s_{ER}}{v_{cyt}} W. \tag{14}$$

## NUMERICAL METHODS

The membrane model (Eqs. 1 through 6) was numerically integrated using the ROW4D program (Valko and Vajda, 1985) on a Convex C220 computer. The values of the physiological parameters used in the model are presented in Table 1. When other parameter values are used

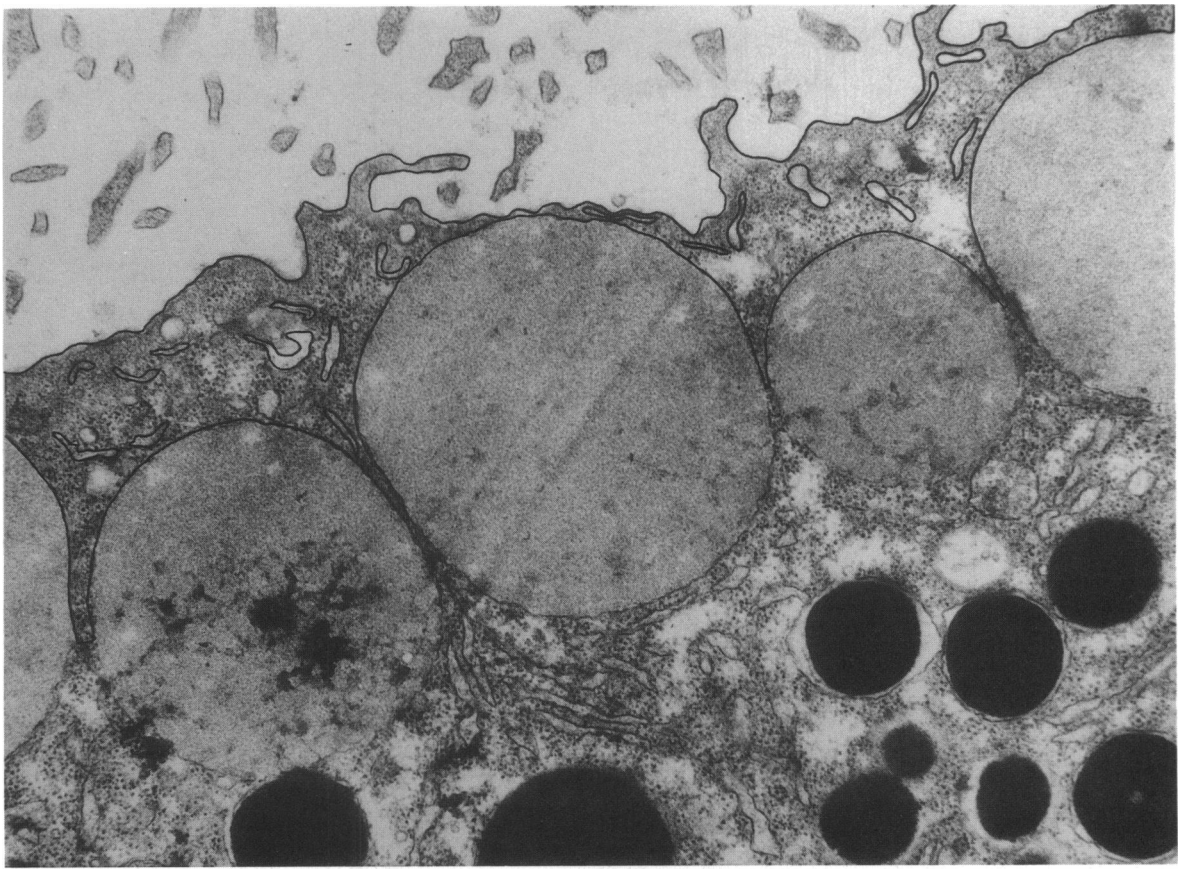

PLATE 1 Electron micrograph of *Xenopus* oocyte (30,000 magnification). The ER structures and cytosolic compartment borders are inked to emphasize the cross-sectional areas that are used in the calculation of the cytosolic compartment volume and the ER surface area.

in the computations they are mentioned in the corresponding figure caption. The value of the calcium entry into the cytosol ($q$) was adjusted to produce the frequency and amplitude of oscillations observed experimentally.

## EXPERIMENTAL RESULTS

### Current fluctuations due to intracellular application of calcium

Shallow injection of calcium into the oocyte ($\sim$100 $\mu$M) evokes a two component chloride current with a fast component that lasts less than a minute and a slow component that appears after 3–4 min (Dascal et al., 1985). The slow component consists of current fluctuations with a small increase in the total current over the base line. However, with increasing the depth of injection ($> \sim$200 $\mu$m) and the injection of a series of small doses, the rapid transient is not detected and more homogenous calcium diffusion in the cell is achieved (Gillo et al., 1987).

All the experiments were performed in calcium-free medium to avoid the effect of the extracellular calcium pool. Fig. 2 *A* shows the response to acute injection (see Methods) of 100 pmol of calcium, 200 $\mu$m below the cell surface membrane. After a delay of $\sim$2 min, the spike-like calcium-induced chloride current appears. The mean interval between the single spikes is 20–30 s. A series of spikes on a slow time base can be seen in Fig. 3 *A*. In Fig. 2 *B*, a series of calcium injections is applied to the oocyte to bring in a total of 400 pmol; the frequency

**TABLE 1 Parameter values for the model**

| Parameter | | Value |
|---|---|---|
| $C_m$ | = | 1 $\mu$F cm$^{-2}$ |
| $F$ | = | 96,500 coulombs (mol $e^-$)$^{-1}$ |
| $\overline{g_{Ca}}$ | = | 340 $\mu$S cm$^{-2}$ |
| $K_{diss}$ | = | 5 $\mu$M |
| $k_{pump}$ | = | 20.2 s$^{-1}$ |
| $k$ | = | 69.8 s$^{1}$ |
| $S$ | = | $6.16 \times 10^{-3}$ cm$^2$ |
| $V_{cyt}$ | = | $5.84 \times 10^{-5}$ $\mu$l |
| $q$ | = | $2.92 \times 10^{-10}$ $\mu$mol s$^{-1}$ |
| $P_{total}$ | = | 120 $\mu$M |
| $k_{off}$ | = | 5 s$^{-1}$ |
| $k_{on}$ | = | 1 $\mu$M$^{-1}$ s$^{-1}$ |
| $[Ca]_{ER}$ | = | 5,000 $\mu$M |
| $V_0$ | = | 12.9 mV |
| $R$ | = | 8.314 J °K$^{-1}$ mol$^{-1}$ |
| $T$ | = | 300 K |
| $r$ | = | 600 $\mu$m |

These parameters are used in the simulations unless otherwise stated.

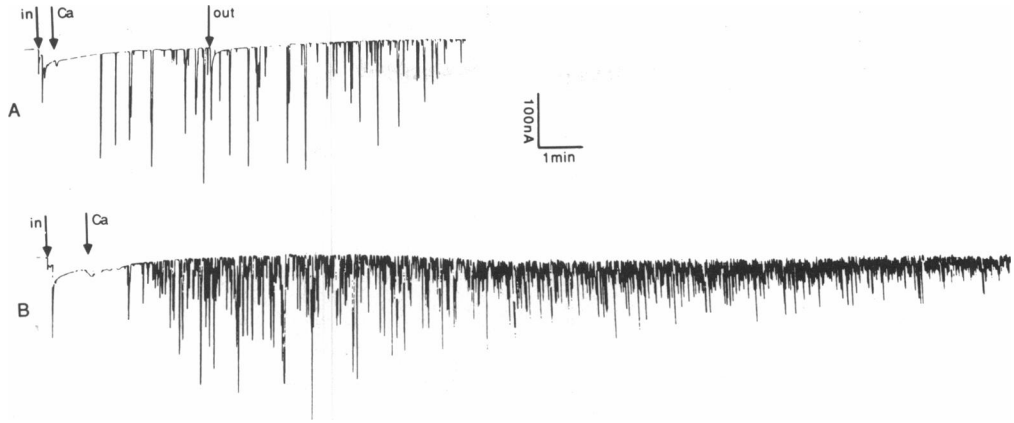


FIGURE 2 Chloride current fluctuations elicited by intracellular injection of calcium in calcium-free medium. The "in" and "out" arrows mark the insertion and withdrawal of the injection pipette. (*A*) A total of 100 pmol of calcium is injected at 200 $\mu$m into the cell. (*B*) A total of 400 pmol of calcium is injected at 200 $\mu$m into the cell in consecutive small doses.

of the oscillations is dramatically increased. As the response progressed, the frequency of the spikes increased and the amplitude decreased, eventually becoming high frequency oscillations. Fig. 3 *B* shows the high frequency low amplitude oscillations on a slow time scale, taken from the same oocyte as in Fig. 2 *B*, 10 min after the injection of calcium. The faster oscillations superimposed on these oscillations are not modelled. The oscillations persist indefinitely; we have recorded for as long as 30 min with no significant diminution of the oscillations. The model suggests that for sustained oscillations there must be a constant calcium flux into the cytosol. This flux is probably due to the sequestration of the initial calcium bolus by intracellular stores and subsequent slow continuous release of calcium from these stores into the cytosol. This also implies that the pumping of calcium out of the cell is relatively small in spite of the fact that the cell is perfused in calcium-free medium. Indeed, Dascal and Boton (1990) reported that repetitive deep injection of calcium into the oocyte loaded the intracellular pool for as long as 90 min.

## Current fluctuations due to extracellular application of calcium

Injection of $IP_3$ or application of calcium-mobilizing neurotransmitter to oocytes increases the cell membrane permeability to calcium either at resting membrane potential (Snyder et al., 1988) or by hyperpolarizing steps (Parker et al., 1987).

Loading the oocyte with a high dose of $IP_3$ (>2 pmol) and maintaining it in calcium-free extracellular medium increase the membrane permeability to calcium for more than an hour. Exposing the cell to a brief (3–5 s) extracellular calcium application evokes a large depolarizing response which results from calcium flux via the open channels. Upon calcium washout, damped current oscillations emerge and decay rapidly (Fig. 4). No calcium oscillations occurred upon longer exposure. However, calcium oscillations are observed after washout. It appears as if the high level of calcium entry into the cytosol attenuates the current oscillations. Thus, we show that cytosolic calcium oscillations can be stimulated by extracellular as well as intracellular application of calcium. Furthermore, no oscillations occur when overloading the cytosol with calcium.

## NUMERICAL RESULTS

We assume that calcium oscillation in *Xenopus* oocytes can be measured by the chloride current across the plasma membrane due to the fact that the chloride channels are calcium gated as shown in studies involving observation of calcium oscillations using a calcium sensitive fluorescent dye and monitoring of the chloride current oscillations (Parker and Miledi, 1986; DeLisle et al., 1990; Parker and Ivorra, 1990). Osipchuk and coworkers (1990) have shown a positive correlation between the cytosolic calcium concentration and the chloride current using microfluorometry and whole cell patch clamp in pancreatic acinar cells. Moreover, the native chloride current seems to better resolve small fluctuations of the cytosolic calcium concentration.

The spikes of our simulated calcium oscillations have a rising phase that is not observed in the chloride current records. This is probably due to a threshold phenomenon. The chloride channels open when the $[Ca]_{cyt}$ reaches a certain threshold level. The existence of the threshold phenomenon has been suggested previously to explain the latency phenomenon (Berridge et al., 1988). The variation in the current records (Fig. 3) might be due to the spatial inhomogeneity of the oscillations (Parker and Ivorra, 1990; Lechleiter et al., 1991). Calcium release from a nearby segment of ER can cause a measurable chloride current that appears in the record as intermediate small oscillations.

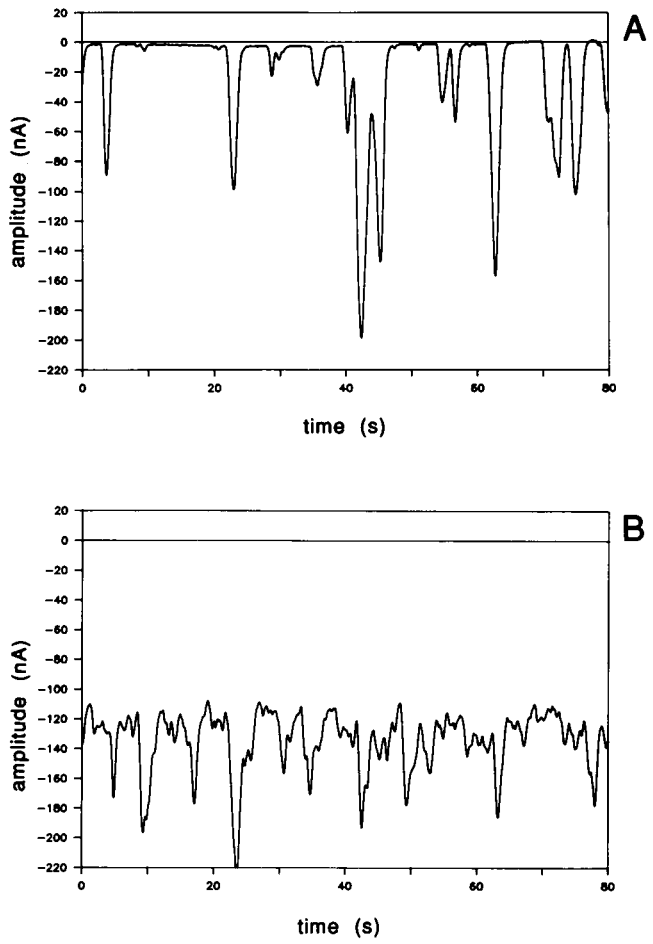


FIGURE 3 Intracellular injection of calcium on an expanded time scale of a current fluctuation. (*A*) Cell injected with a low dose of calcium (100 pmol) exhibits spike-like chloride current fluctuations. (*B*) High frequency current fluctuations observed 10 min after a high dose (400 pmol) calcium injection.

The membrane model reproduces the oscillatory phenomenon observed when calcium is injected into an oocyte. The injection is deep in the oocyte and gradually enters the cortical cytosolic compartment. The model reflects this source of calcium (the flux into the compartment) by the parameter $q$. The ER membrane potential oscillates around its equilibrium value of 89.3 mV (potential difference of the ER lumen to the cytosol). The equilibrium value for the percentage of free calcium binding sites is 95.3%. The equilibrium values are found by solving the system for the dynamic variables when the derivatives are set to zeros (Eqs. 1, 5, and 6). The model reproduces the shape and frequency of oscillations found in *Xenopus* oocytes (Figs. 5 and 6).

Harootunian and co-workers (1988) showed that fibroblasts depolarized by gramicidin, which allows calcium entry into the cell via voltage gated calcium channels, have an increasing frequency and decreasing amplitude of oscillations when exposed to increasing concentrations of extracellular calcium. Similarly, increases in extracellular calcium in the heart cause an increase in the frequency of spontaneous calcium oscillations through calcium entry (Stern et al., 1988). We model this phenomenon by increasing the value of $q$, the constant flux into the cytosol. When $q$ is increased the amplitude decreases and the frequency increases. These relationships are shown in Fig. 7. For low values of $q$ the model shows spiking of the calcium concentration (Fig. 5) and for high values of $q$, the oscillations have low amplitude and high frequency. As the value of $q$ rises beyond $3.2 \times 10^{-10}$ $\mu$mol $s^{-1}$, the oscillations cease as they also do when $q$ becomes zero. In fact, DeLisle and co-workers (1990) find that calcium oscillations stop when an oocyte is bathed in 6 mM calcium, and the oscillations resume when the bath concentration is lowered to 0.1 mM. Similarly, Wakui and Petersen (1990) showed that acetylcholine-induced calcium oscillations in pancreatic acinar cells cease to oscillate when the cells are exposed to ionomycin, which floods the cytosol with calcium from the extracellular space, and that the oscillations resume after the ionomycin is removed.

We performed simulations in which the effect of the buffer was removed to show that the oscillations in the model were due to the calcium-dependent calcium release mechanism rather than binding and release from the buffer. This was accomplished by setting the total amount of the buffer, and the $k_{on}$ and $k_{off}$ for the buffer all to zero. The resulting oscillations increased in both amplitude and frequency (Fig. 8). A similar result was obtained in simulations by increasing the total amount of calcium binding sites, $P_{total}$ (Fig. 9). This finding is comparable to that of Petersen and co-workers (1991), who also observed a decrease in the amplitude and frequency of the cytosolic calcium oscillations upon addition of citrate to pancreatic acinar cells as our model would predict.

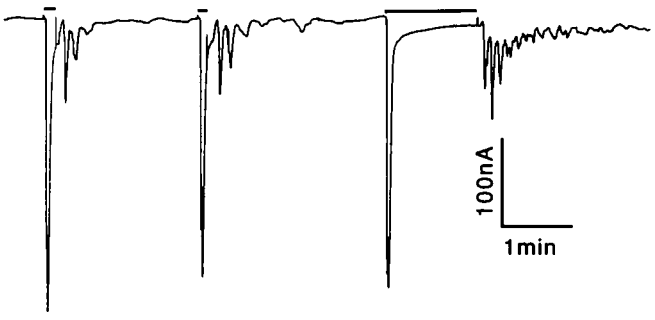


FIGURE 4 Chloride current fluctuation evoked by extracellular application of calcium to an $IP_3$-loaded cell. Oocyte is preloaded with 2.5 pmol $IP_3$. After 15 min, 5 mM Ca is applied during the period indicated by the horizontal bars. The current fluctuations die rapidly with calcium washout. Note that in the third application, when calcium is applied for an extended period, the oscillations cease and reappear after washout.

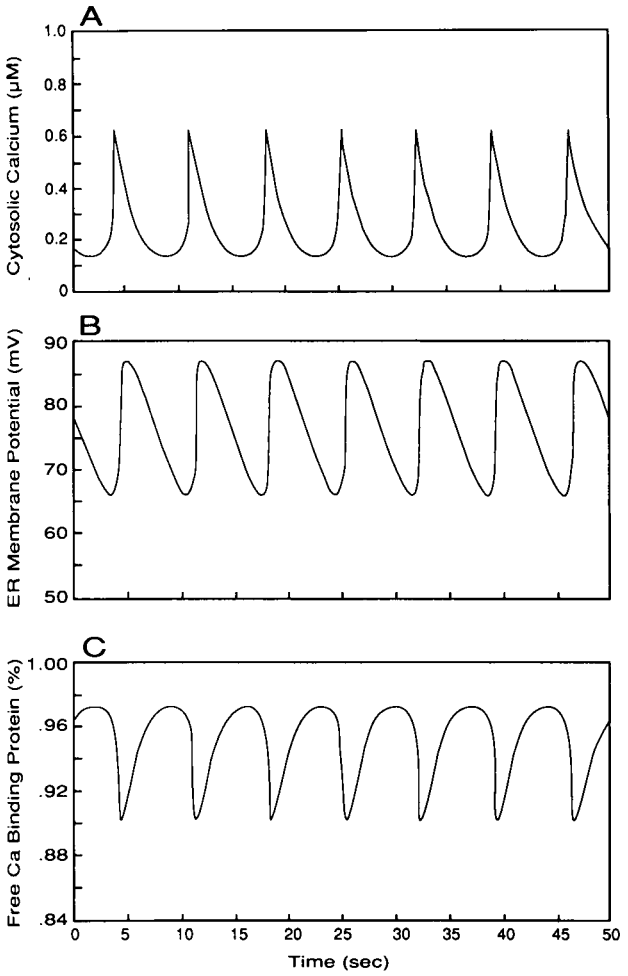


FIGURE 5 Simulation of intracellular calcium injection induced oscillations of (*A*) $[Ca]_{cyt}$, (*B*) ER membrane potential, and (*C*) percentage free calcium binding sites on calcium binding protein for a small constant flux of calcium into the cytosol ($q = 3.21 \times 10^{-10}$ μmol/s).

## DISCUSSION

A system of mathematical equations describing an oscillatory phenomenon arbitrarily far from equilibrium was established to explain a group of oscillating chemical reactions (Prigogine, 1968; Lavenda et al., 1971; Lefever and Nicolis, 1970). A model of this type includes the following mathematical features: a positive feedback term for the oscillating species, a constant flux of this species, a species dependent removal term, and a balance equation for a second species that becomes small when the first species becomes large.

Earlier classes of models for cytosolic calcium oscillations, namely the molecular model (Meyer and Stryer, 1988; Swillens and Mercan, 1990) and the compartmental calcium-exchange model (Kuba and Takeshita, 1981; Goldbeter et al., 1990; Somogyi and Stucki, 1991), result in mathematical formulations that include the features discussed in the preceding paragraph. The main differences between the two classes are the physiological assumptions that determine the meaning of the terms in the differential equations. The dynamic variables in the molecular model are the $[Ca]_{cyt}$ and the cytosolic $IP_3$ concentration, that is, it assumes that the cytosolic calcium as well as the cytosolic $IP_3$ levels are changing. However, cytosolic calcium oscillations are observed in pancreatic acinar cells (Wakui et al., 1990) and in *Xenopus* oocytes (Taylor et al., 1988; DeLisle et al., 1990) injected with a nondegradable analogue of $IP_3$. This suggests that, in a large number of preparations, the cytosolic $IP_3$ concentration remains relatively constant during the calcium oscillations and, therefore, the latter cannot be explained by $IP_3$ fluctuations. Furthermore, cytosolic calcium oscillations in hepatocytes are independent of $IP_3$ formation (Rooney et al., 1991).

$IP_3$ is believed to cause calcium release from intracellular stores. We propose that the constant level of $IP_3$ causes a constant release of calcium, which results in the

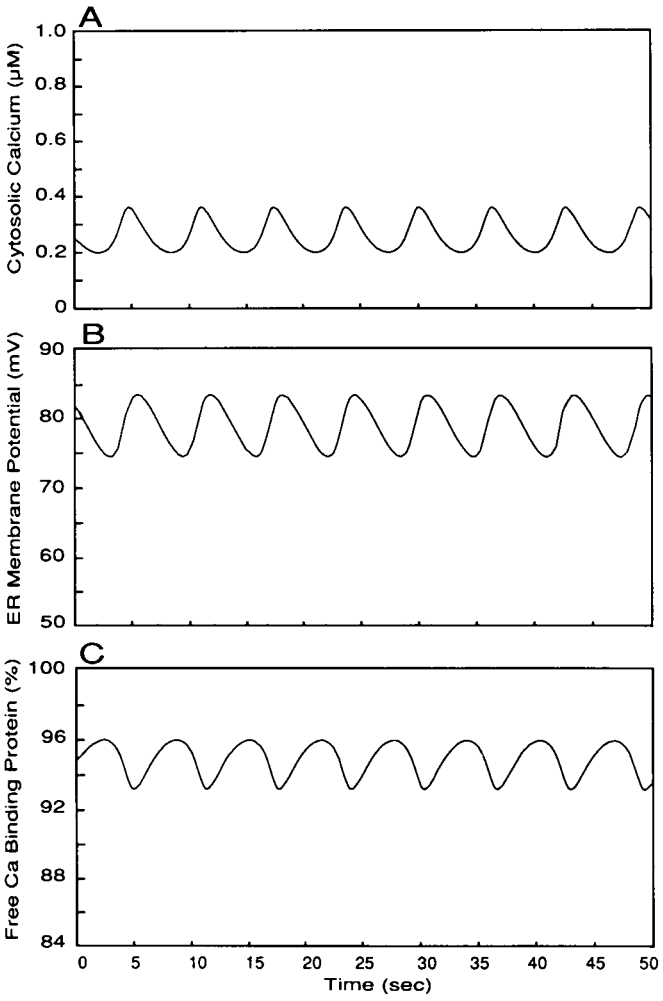


FIGURE 6 Simulation of intracellular calcium injection induced oscillations of (*A*) $[Ca]_{cyt}$ and (*B*) ER membrane potential, and (*C*) percentage free calcium binding sites on calcium binding protein for a large constant flux of calcium into the cytosol ($q = 2.77 \times 10^{-10}$ μmol $s^{-1}$).

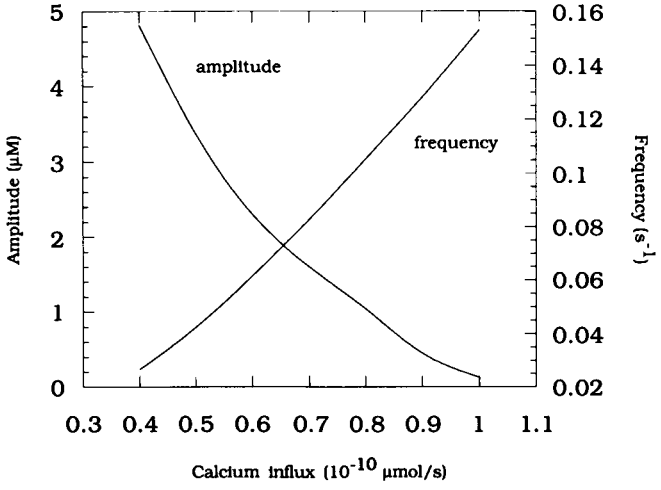


FIGURE 7 The effects of varying the constant flux into the cytosol ($q$) on the amplitude and frequency of the oscillations in cytosolic calcium.

occurrence of oscillations. Similarly, direct intracellular or extracellular application of calcium allows calcium entry into the cell cytosol which generates cytosolic calcium oscillations. The calcium entry from both sources is described by the constant flux $q$ in the differential equations.

The dynamic variables of the compartmental calcium-exchange model (Goldbeter et al., 1990) are the

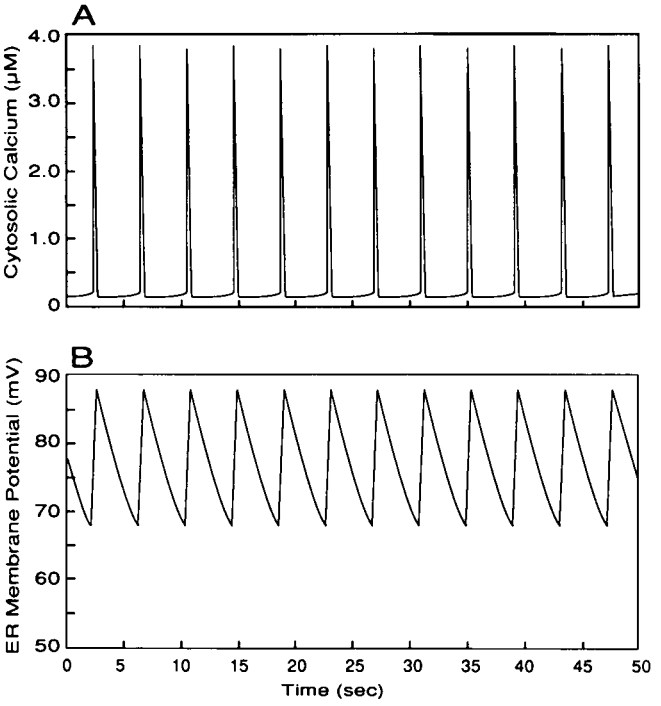


FIGURE 8 Simulation of the oscillations in ($A$) $[Ca]_{cyt}$ and ($B$) ER membrane potential after removal of the buffer ($P_{total}$) = 0, $k_{on}$ = 0, and $k_{off}$ = 0). Note the increase in the amplitude and frequency of the oscillations.

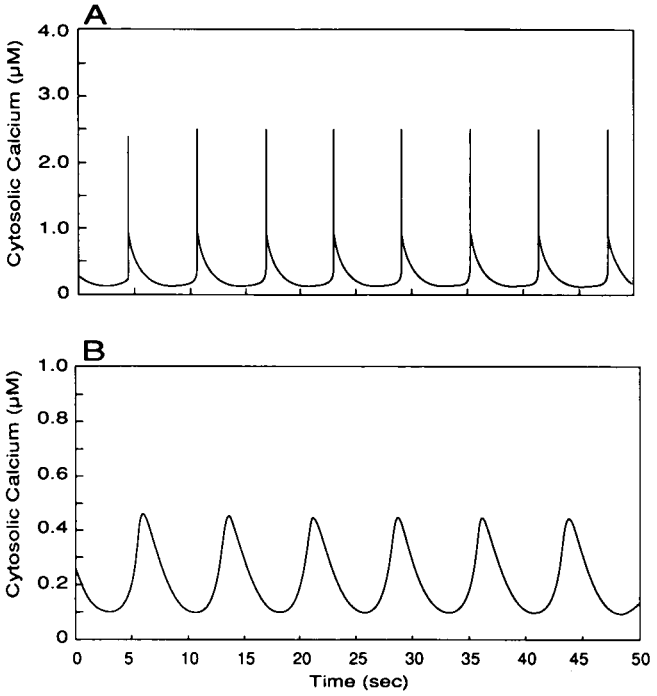


FIGURE 9 Simulation of the calcium oscillations with different concentrations of calcium binding sites: ($A$) 80 μM and ($B$) 140 μM. Note that with increased buffer the oscillations have a decreased amplitude and frequency.

cytosolic calcium concentration and the ER luminal calcium concentration. In this model, the positive feedback for calcium (Ca-dependent Ca release channel) is activated by a rise in calcium in both the cytosol and the ER lumen. The channel is closed by depletion of the $[Ca]_{ER}$. This, however, conflicts with the finding of Lai and coworkers (1988) that SR luminal calcium has no effect on the duration for which a channel stays in the open state. In contrast, our membrane model uses the reduction of the electrochemical gradient to terminate the calcium release from the ER.

Electron microprobe analysis has shown that during tetanic contraction in skinned striated muscle, magnesium and potassium ions move into the sarcoplasmic reticulum (SR), and calcium is released (Somlyo et al., 1981). Although the contribution of these counterions is not insignificant, they together have about half the charge of the calcium ions. For simplicity, the present model considers only the contribution of the calcium ions because adding the potassium and magnesium ions would involve the addition of two more dynamic variables to our model. This omission may not be critical to the qualitative behavior of the model because the counterion effect serves to maintain an electrochemical gradient that allows calcium release down the gradient. This discrepancy can be later modelled as the contribution of other ions distributed across the membrane to establish the resting potential. More information on their move-

ment is needed to firmly establish their role, if any, in cytosolic calcium oscillations.

Our model demonstrates the local temporal behavior of cytosolic calcium concentration. It does not describe the spatial inhomogeneity. A possible direction for further research is to model the spatial properties of the oscillations. For example, calcium released from the ER can trigger calcium-dependent calcium release in the adjacent ER and hence calcium release can be propagated along the sheets of ER as shown by Lechleiter and co-workers (1991) in *Xenopus* oocytes.

As an initial test of the membrane model we studied the calcium-evoked chloride current oscillations in *Xenopus* oocytes. The experiment was performed in calcium-free medium to exclude the effect of an extracellular calcium source. In response to an injection of a low calcium dose, the current oscillations were high amplitude, low frequency spikes. A high dose initially elicited high frequency spikes. As time progressed, the oscillations increased in frequency with a decreased amplitude. These changes in the behavior of the calcium oscillations can be modelled by an increase in the calcium entry into the compartment, represented by $q$. Considering the large dose of calcium necessary to evoke oscillations (0.1–0.4 mM final concentration) and the elimination of the fast component (Fig. 2), we infer that most of the calcium is sequestered into the intracellular stores and by calcium binding proteins before oscillations begin. With no other source of calcium we propose that the gradual conversion from transient spikes to high frequency oscillations results from overloading of the pumps or depletion of ATP which leads to an increase in $[Ca]_{cyt}$ via increased calcium entry into the oscillatory cytosolic compartment. The same mechanism has been recently proposed for potentiation of the calcium evoked chloride current by repetitive calcium injection in *Xenopus* oocytes (Dascal and Boton, 1990). Similarly, Wakui and co-workers (1990) obtained calcium oscillations in pancreatic acinar cells by infusion of 100 $\mu$M calcium.

The model predicts that as calcium entry into the cytosol increases, the oscillation frequency increases and its amplitude decreases. This is supported by a similar observation in fibroblasts depolarized by gramicidin (Harootunian et al., 1988) and exposed to extracellular calcium and in cardiac myocytes exposed to extracellular calcium (Stern et al., 1988). Gillo and co-workers (1987) showed that shallow injection of $IP_3$ (high local dose) produced very small oscillations compared with deep injection (low dose; see also above). The same relationship is observed in a response to a calcium-mobilizing hormone in RNA-injected oocytes (gonadotropin releasing hormone; S. Sealfon, personal communication). Moreover, the transition from sinusoidal-like to transient spiking behavior for the oscillations can be achieved by decreasing $q$. The various forms of oscillations that appear in a variety of preparations have been reviewed recently (Berridge and Irvine, 1989; Rooney and Thomas, 1991). Furthermore, the model predicts that when the constant calcium entry is too small or too large no oscillations will occur.

When the total amount of calcium binding sites is increased (and $q$ is held constant) the calcium oscillations decrease in amplitude and frequency. The decrease in amplitude occurs because the calcium released from the ER is sequestered by the additional buffer. The fall in frequency occurs because the rise of cytosolic calcium to threshold is slower due to the increased buffering effect, that is, there is a smaller increase in free cytosolic calcium. This threshold is the point at which calcium-dependent calcium release becomes the predominant process. This finding is supported by the work of Petersen and co-workers (1991). When citrate is added to pancreatic acinar cells the amplitude and frequency of the cytosolic calcium oscillations decrease. Our model predicts that removal of buffer will result in an increase of amplitude and frequency of the oscillations. In addition, with a decrease in amount of buffer, the form of the oscillations will change from sinusoidal to a transient spiking pattern.

Oscillations are observed in $IP_3$ loaded cells exposed to extracellular calcium. $IP_3$ loading increases the plasmalemmal permeability to calcium. This shows that the source of calcium flux can be extracellular as well as intracellular.

The model demonstrates that a constant calcium entry into the cytosol is sufficient for the occurrence of oscillations. Moreover, this flux serves as a mechanism by which the frequency and amplitude can be regulated. The source of calcium can be the result of numerous physiological origins such as $IP_3$ mediated release, flux from external sources, etc. The degree of binding of calcium by intracellular calcium binding proteins can also regulate the form, amplitude, and frequency of cytosolic calcium oscillations. These two factors can be used in concert to reproduce a wide variety of oscillations. This suggests a possible mechanism by which a cell can produce the different types of oscillations described in the review by Rooney and Thomas (1991).

The membrane model demonstrates that the salient features needed to produce cytosolic calcium oscillations are calcium-dependent calcium release, a calcium-dependent removal, and a source of constant calcium entry. In order to extend the model to simulate calcium oscillations observed in various cells or under different conditions, the differential equations might be further developed to include terms for other observed physiological mechanisms for calcium regulation. Further experimentation is needed to validate the physiological assumptions that define the model.

We are greatly thankful to S. Mundamattom who performed the electrophysiological experiments. We would like to give special thanks to Dr. S. C. Sealfon and Dr. A. Sherman for their helpful remarks and discussion.

## REFERENCES


Ambler, S. K., P. Poenie, R. Y. Tsien, and P. Taylor. 1988. Agonist-stimulated oscillations and cycling of intracellular free calcium in individual cultured muscle cells. *J. Biol. Chem.* 263:1952–1959.

Benham, C. D., and T. B. Bolton. 1986. Spontaneous transient outward currents in single visceral and vascular smooth muscle cells of the rabbit. *J. Physiol. (Lond.).* 381:385–406.

Berridge, M. J., P. H. Cobbold, and K. S. R. Cuthbertson. 1988. Spatial and temporal aspects of cell signalling. *Phil. Trans. R. Soc. Lond. B.* 320:325–343.

Berridge, M. J., and R. F. Irvine. 1989. Inositol phosphate and cell signalling. *Nature (Lond.).* 341:197–205.

Cartaud, A., R. Ozon, M. P. Walsh, J. Haiech, and J. G. Demaille. 1980. *Xenopus Laevis* oocyte calmodulin in the process of meiotic maturation. *J. Biol. Chem.* 255:9404–9408.

Charbonneau, M., and R. D. Grey. 1984. The onset of activation responsiveness during maturation coincides with the formation of the cortical endoplasmic reticulum in oocytes of *Xenopus laevis. Dev. Biol.* 102:90–97.

Chay, T. R., and J. Keizer. 1983. Minimal model for membrane oscillations in the pancreatic β-cell. *Biophys. J.* 42:181–190.

Dascal, N., and R. Boton. 1990. Interaction between injected $Ca^{2+}$ and intracellular $Ca^{2+}$ stores in *Xenopus* oocytes. *FEBS Lett.* 267:22–24.

Dascal, N., B. Gillo, and Y. Lass. 1985. Role of calcium mobilization in mediation of acetylcholine responses in *Xenopus laevis* oocytes. *J. Physiol. (Lond.).* 366:299–314.

Delesse, M. A. 1847. Procede mecanique pour determiner la composition des roches. *Comput. Rend. Acad. Sci.* 25:544–547.

DeLisle, S., K. Krause, G. Denning, B. V. L. Potter, and M. J. Welsh. 1990. Effect of inositol trisphosphate and calcium on oscillation elevations of intracellular calcium in *Xenopus* oocytes. *J. Biol. Chem.* 265:11726–11730.

Dumont, J. N. 1972. Oogenesis in *Xenopus laevis* (Daudin). *J. Morphol.* 136:153–180.

Gandhi, C. R., and D. H. Ross. 1988. Characterization of a high-affinity $Mg^{2+}$-independent $Ca^{2+}$-ATPase from rat brain synaptosomal membranes. *J. Neurochem.* 50:248–256.

Gardiner, D. M., and R. D. Grey. 1983. Membrane junctions in *Xenopus* eggs: their distribution suggests a role in calcium regulation. *J. Cell Biol.* 96:1159–1163.

Gillo, B., Y. Lass, E. Nadler, and Y. Oron. 1987. The involvement of inositol 1,4,5-trisphosphate and calcium in the two-component response to acetylcholine in *Xenopus* oocytes. *J. Physiol. (Lond.).* 392:349–361.

Goldbeter, A., G. Dupont, and M. J. Berridge. 1990. Minimal model for signal induced $Ca^{2+}$ oscillations and for their frequency encoding through protein phosphorylation. *Proc. Natl. Acad. Sci. USA.* 87:1461–1465.

Gray, P. T. A. 1988. Oscillations of free cytosolic calcium evoked by cholinergic and catecholaminergic agonists in rat parotid acinar cells. *J. Physiol. (Lond.).* 406:35–53.

Harootunian, A. T., J. P. Y. Kao, and R. Y. Tsien. 1988. Agonist-induced calcium oscillations in depolarized fibroblasts and their manipulation by photoreleased $Ins(1,4,5)P_3$, $Ca^{++}$, and $Ca^{++}$ buffer. *Cold Spring Harbor Symp. Quant. Biol.* 53:935–943.

Jacob, R., J. E. Merritt, T. J. Hallam, and T. J. Rink. 1988. Repetitive spikes in cytoplasmic calcium evoked by histamine in human endothelial cells. *Nature (Lond.).* 335:40–45.

Kuba, K., and Takeshita. 1981. Simulation of intracellular $Ca^{2+}$ oscillations in a sympathetic neurone. *J. Theor. Biol.* 93:1009–1031.

Lai, F. A., H. P. Erickson, E. Rosseau, Q. Liu, and G. Meissner. 1988. Purification and reconstitution of the calcium release channel from skeletal muscle. *Nature (Lond.).* 331:315–319.

Lakatta, E. G., M. C. Capogrossi, A. A. Kort, and M. D. Stern. 1986. Spontaneous myocardial calcium oscillations: overview with emphasis on ryanodine and caffeine. *Fed. Proc.* 44:2977–2983.

Lavenda, B., G. Nicolis, and M. Herschkowitz-Kaufman. 1971. Chemical instabilities and relaxation oscillations. *J. Theor. Biol.* 32:283–292.

Lechleiter, J., S. Girard, E. Peralta, and D. Clapham. 1991. Spiral calcium wave propagation and annihilation in *Xenopus laevis* oocytes. *Science (Wash. DC).* 252:123–126.

Lefever, R., and G. Nicolis. 1970. Chemical instabilities and sustained oscillations. *J. Theor. Biol.* 30:267–284.

Lin N. Y., Y. P. Liu, and W. Y. Cheung. 1974. Cyclic 3':5'-nucleotide phosphodiesterase: purification, characterization, and active form of the protein activator from bovine brain. *J. Biol. Chem.* 249:4943–4954.

Meissner, G., E. Darling, and J. Eveleth. 1986. Kinetics of rapid $Ca^{2+}$ release by sarcoplasmic reticulum. Effects of $Ca^{2+}$, $Mg^{2+}$, and adenine nucleotides. *Biochemistry.* 25:236–244.

Meyer, T., and L. Stryer. 1988. Molecular model for receptor-stimulated calcium spiking. *Proc. Natl. Acad. Sci. USA.* 85:5051–5055.

Ogawa, Y., N. Kurebayashi, A. Irimajiri, and T. Hanai. 1981. Transient kinetics for Ca uptake by fragment sarcoplasmic reticulum from bullfrog skeletal muscle with reference to the rate of relaxation in living muscle. *Adv. Physiol. Sci.* 5:417–435.

Okada, Y., W. Tsuchiya, and T. Yada. 1982. Calcium channel and calcium pump involved in oscillatory hyperpolarizing responses of L-strain mouse fibroblasts. *J. Physiol. (Lond.).* 327:440–461.

Osipchuk, Y. V., M. Wakui, D. I. Yule, D. V. Gallacher, and O. H. Petersen. 1990. Cytoplasmic $Ca^{2+}$ oscillations evoked by receptor stimulation, G-protein activation, internal application of inositol trisphosphate of $Ca^{2+}$: simultaneous microfluorometry and $Ca^{2+}$ dependent $Cl^-$ current recording in single pancreatic acinar cells. *EMBO J.* 9:697–704.

Parker, I., and I. Ivorra. 1990. Localized all-or-none calcium liberation by inositol trisphosphate. *Science (Wash. DC).* 250:977–979.

Parker, I., and R. Miledi. 1986. Changes in intracellular calcium and in membrane currents evoked by injection of inositol trisphosphate into *Xenopus* oocytes. *Proc. R. Soc. Lond. B.* 228:307–315.

Parker, I., K. Sumikawa, and R. Miledi. 1987. Activation of a common effector system by different brain neurotransmitter receptors in *Xenopus* oocytes. *Proc. R. Soc. Lond.* 231:37–45.

Petersen, C. C. H., E. C. Toescu, and O. H. Petersen. 1991. Different patterns of receptor-activated cytoplasmic $Ca^{2+}$ oscillations in single pancreatic acinar cells: dependence on receptor type, agonist concentration and intracellular $Ca^{2+}$ buffering. *EMBO J.* 10:527–533.

Prigogine, I. 1968. Introduction to Thermodynamics of Irreversible Processes. 3rd Ed. Wiley Interscience, New York. 147 pp.

Robertson, S. P., J. D. Johnson, and J. D. Potter. 1981. The time-course of $Ca^{2+}$ exchange with calmodulin, troponin, parvalbumin, and myosin in response to transient increases in $Ca^{2+}$. *Biophys. J.* 34:559–569.

Rooney, T. A., D. C. Renard, E. J. Sass, and A. P. Thomas. 1991. Oscillatory cytosolic calcium waves independent of stimulated inositol 1,4,5-trisphosphate formation in hepatocytes. *J. Biol. Chem.* 266:12272–12282.

Rooney, T. A., and A. P. Thomas. 1991. Organization of intracellular calcium signals generated by inositol lipid-dependent hormones. *Pharmac. Ther.* 49:223–237.

Schlegal, W., B. P. Winger, P. Mollard, F. Wuarin, G. R. Zahnd, C. B. Wolheim, and B. Dufy. 1987. Oscillations of cytosolic $Ca^{2+}$ in pituitary cells due to action potentials. *Nature (Lond.).* 329:719–721.

Snyder, P. M., K. H. Krause, and M. J. Welsh. 1988. Inositol trisphosphate isomers, but not inositol 1,3,4,5 tetrakisphosphate, induces

calcium influx in *Xenopus laevis* oocytes. *J. Biol. Chem.* 263:11048–11051.

Somlyo, A. V., H. Gonzalez-Serratos, H. Shuman, G. McClellan, and A. P. Somlyo. 1981. Calcium release and ionic changes in the sarcoplasmic reticulum of tetanized muscle: an electron-probe study. *J. Cell Biol.* 90:577–594.

Somogyi, R., and J. W. Stucki. 1991. Hormone-induced calcium oscillations in liver cells can be explained by a simple one pool model. *J. Biol. Chem.* 266:11068–11077.

Stern, M. D., M. C. Capogrossi, and E. G. Lakatta. 1988. Spontaneous calcium release from the sarcoplasmic reticulum in myocardial cells: mechanisms and consequences. *Cell Calcium.* 9:247–258.

Swillens, S., and D. Mercan. 1990. Computer simulation of a cytosolic calcium oscillator. *Biochem. J.* 271:835–838.

Takahashi, T., E. Neher, and B. Sakmann. 1987. Rat brain serotonin receptors in *Xenopus* oocytes are coupled by intracellular calcium to endogenous channels. *Proc. Natl. Acad. Sci. USA.* 84:5063–5067.

Taylor, W. C., W. J. Berridge, K. D. Brown, A. M. Cooke, and B. V. L. Potter. 1988. Dl-myo-inositol 1,4,5-trisphosphate mobilizes intracellular calcium in Swiss 3T3 cells and *Xenopus* oocytes. *Biochem. Biophys. Res. Commun.* 150:626–632.

Valko, P., and S. Vajda. 1985. An extended ODE solver for sensitivity calculations. *Comput. Chem.* 8:255–271.

Wakui, M., Y. V. Osipchuk, and O. H. Petersen. 1990. Receptor-activated cytoplasmic $Ca^{2+}$ spiking mediated by inositol trisphosphate is due to $Ca^{2+}$-induced $Ca^{2+}$ release. *Cell.* 63:1025–1032.

Wakui, M., and O. H. Petersen. 1990. Cytoplasmic $Ca^{2+}$ oscillations evoked by acetylcholine or intracellular infusion of inositol trisphosphate or $Ca^{2+}$ can be inhibited by internal $Ca^{2+}$. *FEBS Lett.* 263:206–208.

Wakui, M., V. L. Potter, and O. H. Petersen. 1989. Pulsatile intracellular calcium release does not depend on fluctuations in inositol trisphosphate concentration. *Nature (Lond.).* 339:317–320.

Wolff, D. J., P. G. Poirier, C. O. Brostrom, and M. A. Brostrom. 1977. Divalent cation binding properties of bovine brain $Ca^{2+}$-dependent regulator protein. *J. Biol. Chem.* 252:4108–4117.